

## “Magic Melters” Have Geometrical Origin

Kavita Joshi, Sailaja Krishnamurty, and D. G. Kanhere

Department of Physics and Center for Modeling and Simulation, University of Pune, Ganeshkhind, Pune-411 007, India

(Received 30 December 2005; published 7 April 2006)

Recent experimental reports bring out extreme size sensitivity in the heat capacities of gallium and aluminum clusters. In the present work we report results of our extensive *ab initio* molecular dynamical simulations on  $\text{Ga}_{30}$  and  $\text{Ga}_{31}$ , the pair which has shown rather dramatic size sensitivity. We trace the origin of this size sensitive heat capacities to the relative order in their respective ground state geometries. Such an effect of nature of the ground state on the characteristics of heat capacity is also seen in case of small gallium and sodium clusters, indicating that the observed size sensitivity is a generic feature of small clusters.

DOI: [10.1103/PhysRevLett.96.135703](https://doi.org/10.1103/PhysRevLett.96.135703)

PACS numbers: 64.70.Nd, 36.40.Ei, 65.40.Ba, 82.20.Wt

The finite temperature behavior of clusters has shown many interesting and intriguing properties [1–5]. Recently, the calorimetric measurements reported by Jarrold and co-workers found that small clusters of tin and gallium in the size range of 17–55 atoms have *higher than bulk* melting temperatures ( $T_{m[\text{bulk}]}$ ) [2,3]. A striking experimental result from the same group showed extreme size sensitivity in the nature of the heat capacity for Ga clusters in the size range of 30–55 atoms [4]. It turns out that the addition of even one atom changes the heat capacity dramatically. For example,  $\text{Ga}_{30}^+$  has a rather flat specific heat curve, whereas the heat capacity of  $\text{Ga}_{31}^+$  has a well-defined peak and has been termed “magic melter.” A similar size sensitive feature has also been observed in the case of Al clusters [5].

The explanation and understanding of various experimental observations have come from the first-principles density functional (DF) simulations [6–10]. For example, the higher than bulk melting temperature for Sn and Ga clusters is understood as being due to the difference in the nature of bonding between the cluster and the bulk [6,8,10]. However, the extreme size sensitivity displayed in gallium and aluminum clusters is still an unexplained phenomena. The present work addresses this issue by employing first-principles DF methods. In this Letter we report our results of *ab initio* molecular dynamical (MD) simulations carried out on  $\text{Ga}_{30}$  and  $\text{Ga}_{31}$ . It is of some interest to note that similar size sensitive heat capacities have been observed in case of  $\text{Ga}_n$  ( $n = 17, 20$ ) [9] and  $\text{Na}_n$  ( $n = 40, 50, 55$ ) [11] clusters. In both these cases the addition of a few atoms changes the nature of heat capacities significantly. By analyzing the geometry of the ground state, we establish a definitive correlation between the nature of the ground state and the observed heat capacity. Our detailed calculations show that an “ordered” ground state leads to a heat capacity with a well-defined peak, while a cluster with “disordered” ground state leads to a flat heat capacity with no distinct melting transition. In what follows we will make the meaning of “order” and “disorder” precise and provide an explanation for the size sensitive heat capacities.

We have carried out constant temperature Born-Oppenheimer MD simulations using ultrasoft pseudopotentials within the generalized gradient approximation [12]. For all the clusters reported here we have obtained at least 200 equilibrium structures. For computing heat capacities of  $\text{Ga}_{30}$  and  $\text{Ga}_{31}$  the MD calculations were carried out for 16 different temperatures, each with the duration of 150 ps or more, in the range of  $100 \leq T \leq 1100$  K, which results in a total simulation time of 2.4 ns. In order to get converged heat capacity curves especially in the region of coexistence, more temperatures were required with longer simulation time. The resulting trajectory data have been used to compute the ionic specific heat by employing the multiple histogram method [13,14].

Figure 1 shows the calculated heat capacity of  $\text{Ga}_{30}$  and  $\text{Ga}_{31}$ . Evidently the dramatic difference in the heat capacities of  $\text{Ga}_{30}$  and  $\text{Ga}_{31}$  observed in the experiments is well reproduced in our simulations. Thus  $\text{Ga}_{31}$  has a well-defined peak in the heat capacity, whereas the heat capacity for  $\text{Ga}_{30}$  is rather flat. We also note that both  $\text{Ga}_{30}$  and  $\text{Ga}_{31}$

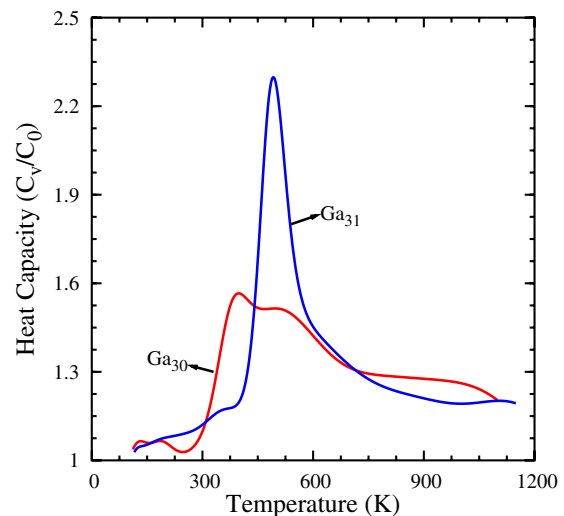


FIG. 1 (color online). The heat capacity of  $\text{Ga}_{31}$  and  $\text{Ga}_{30}$  computed over 90 ps.

become “liquidlike” at temperatures much higher than  $T_{m[\text{bulk}]}$  (303 K), i.e., above 500 K, consistent with the experiments. In order to gain insight into these observations, we analyze the ground state of  $\text{Ga}_{30}$  and  $\text{Ga}_{31}$ . In Fig. 2 we show the ground state geometries of  $\text{Ga}_{30}$  and  $\text{Ga}_{31}$  with two different perspectives. A cursory analysis of Fig. 2(a) may lead to the conclusion that the only difference between  $\text{Ga}_{30}$  and  $\text{Ga}_{31}$  ground states is the presence of the capped atom in  $\text{Ga}_{31}$ . However, a different view obtained by rotating the cluster by  $90^\circ$  brings out the significant differences in  $\text{Ga}_{30}$  and  $\text{Ga}_{31}$ , clearly indicating that  $\text{Ga}_{31}$  is more ordered. A careful examination of Fig. 2(b) shows the presence of well-ordered planes in  $\text{Ga}_{31}$ . Such planes are only in a formative stage and considerably deformed in  $\text{Ga}_{30}$ . In fact, an addition of just one atom in  $\text{Ga}_{30}$  displaces *all* the atoms by a significant amount which makes  $\text{Ga}_{31}$  more ordered. That a single atom makes a substantial rearrangement is also seen by the fact that there is a noticeable difference in the coordination number of atoms in these two clusters. In Fig. 3 we show the number of atoms as a function of the coordination number. It can be noted that in  $\text{Ga}_{30}$ , 5 atoms have 4 or more coordination number, whereas in  $\text{Ga}_{31}$ , 14 atoms have fourfold or higher coordination. Therefore we term  $\text{Ga}_{30}$  as a disordered structure relative to  $\text{Ga}_{31}$ .

Thus when the system is disordered, each atom (possibly a group of atoms) is likely to have different local environment. That means different atoms are bonded with the rest of the system with varying strength. Consequently, their dynamical behavior as a response to temperature will differ. Some of the atoms may pick up kinetic energy at

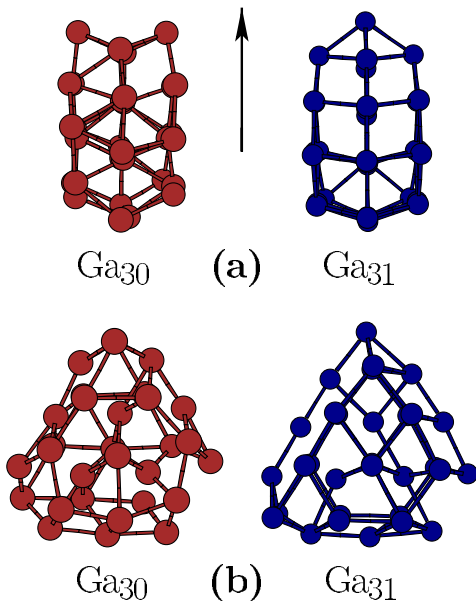


FIG. 2 (color online). The ground state geometry of  $\text{Ga}_{30}$  and  $\text{Ga}_{31}$  with two different perspectives. Perspective (b) is rotated by  $90^\circ$  with respect to perspective (a) about an axis shown in the figure.

low temperatures, while the others may do so at higher temperatures. In a given structure, if a large group of atoms are bonded together with a similar strength forming an island of local order, it is reasonable to expect that they will “melt” together. In this case the cluster can be considered as (at least partially) ordered and will show a well-defined peak in the heat capacity. However, if the system is disordered in the sense that there are no such islands of significant sizes having local order, then we expect a very broad continuous phase transformation. Indeed, our analysis of mean square displacement (MSD) for individual atoms brings out this fact clearly. The MSD for individual atoms is defined as

$$\langle \mathbf{r}_I^2(t) \rangle = \frac{1}{M} \sum_{m=1}^M [\mathbf{R}_I(t_{0m} + t) - \mathbf{R}_I(t_{0m})]^2, \quad (1)$$

where  $\mathbf{R}_I$  is the position of the  $I$ th atom and we average over  $M$  different time origins  $t_{0m}$  spanning the entire trajectory. In Fig. 4 we show MSDs of individual atoms for  $\text{Ga}_{30}$  and  $\text{Ga}_{31}$  at 250 K. The contrast between the kinetic response of individual atoms in  $\text{Ga}_{30}$  and  $\text{Ga}_{31}$  is very clear. For  $\text{Ga}_{30}$ , the MSDs of individual atoms show that at least 10 atoms have picked up more kinetic energy compared to other atoms and hence have significantly higher displacements ( $9.0 \text{ \AA}^2$  as compared to  $0.45 \text{ \AA}^2$ ), whereas in  $\text{Ga}_{31}$  all atoms are oscillating about their mean positions and exhibit small values of MSDs ( $0.45 \text{ \AA}^2$ ). Thus MSDs clearly indicate that in  $\text{Ga}_{30}$  different atoms have different mobilities at low temperatures. This wide distribution of MSDs in  $\text{Ga}_{30}$  indicates that the cluster is in coexistence phase around 250 K and is continuously evolving. This is precisely what is expected if the cluster is disordered in the sense described above. This

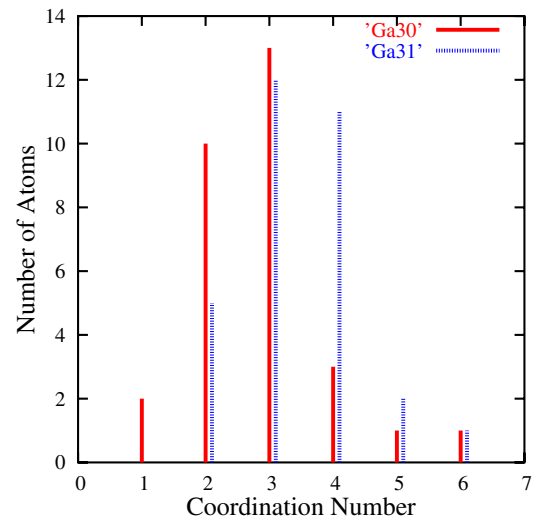


FIG. 3 (color online). Coordination numbers for  $\text{Ga}_{30}$  and  $\text{Ga}_{31}$ . We note that in  $\text{Ga}_{30}$  most of the atoms have either 2 or 3 as a coordination number, whereas in  $\text{Ga}_{31}$  the coordination number is either 3 or 4.

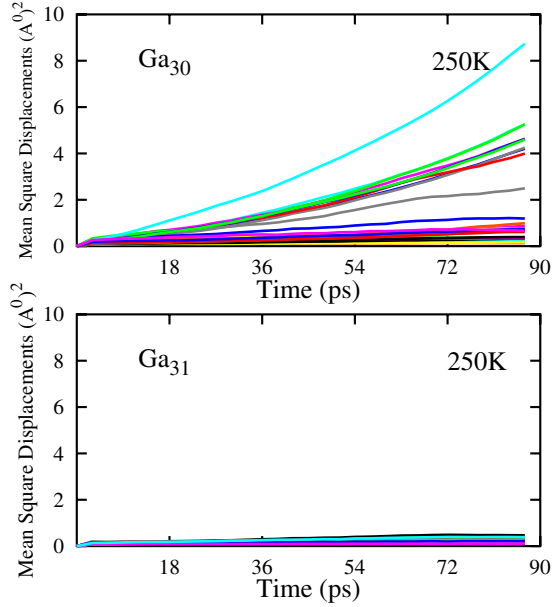


FIG. 4 (color online). The MSD for individual atoms of  $\text{Ga}_{30}$  and  $\text{Ga}_{31}$  computed over 90 ps.

phenomenon has also been observed in the extended systems and a similar analysis has been used to characterize the nature of spatial inhomogeneities with considerable success [15].

The difference in the mobilities of individual atoms in these two clusters is also reflected in the root-mean square bond-length fluctuations ( $\delta_{\text{rms}}$ ) shown in Fig. 5.  $\delta_{\text{rms}}$  shows a clear signal for the beginning of the change of phase around 450 K for  $\text{Ga}_{31}$ . However, in case of  $\text{Ga}_{30}$  the transition is spread over a much broader range of temperatures. In fact, the coexistence region for  $\text{Ga}_{31}$  is over 175 K (from 425 to 600 K), and for  $\text{Ga}_{30}$  it extends over 425 K. It is interesting to note that in  $\text{Ga}_{30}$  the isomerization begins around 175 K and continues till 600 K.

The nature of the order can also be brought out by examining the electron localization function (ELF). The

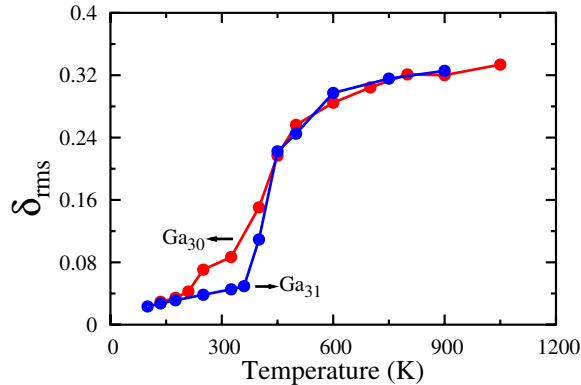


FIG. 5 (color online). The  $\delta_{\text{rms}}$  for  $\text{Ga}_{30}$  and  $\text{Ga}_{31}$  computed over last 90 ps.

ELF has been found to be extremely useful for elucidating the bonding characteristics of a variety of systems [16]. For a single determinantal wave function  $\psi_i$ , the ELF is defined as [17],

$$\chi_{\text{ELF}} = [1 + (D/D_h)^2]^{-1}, \quad (2)$$

where

$$D_h = (3/10)(3\pi^2)^{5/3} \rho^{5/3}, \quad (3)$$

$$D = (1/2) \sum_i |\nabla \psi_i|^2 - (1/8) |\nabla \rho|^2 / \rho, \quad (4)$$

with  $\rho \equiv \rho(\mathbf{r})$  is the valence-electron density. The ELF is defined in such a way that its value is unity for completely localized systems and 0.5 for homogeneous electron gas. It is more convenient to analyze the topology of the ELF surface by using concepts of attractors and their basins [18]. The locations of the maxima of  $\chi_{\text{ELF}}$  are called attractors. A set of all points in space which can be connected to these attractors by maximum gradient paths is called their basins. In the present case the attractors are located at the ionic sites, the ELF being maximum there. For large enough values of ELF, there are as many basins as number of ions. As the value of the ELF is decreased, the basins get connected, and finally at some low value we get a single basin. The value of the ELF at which the basins get connected is a measure of the strength of interaction between the different atoms. This means that the number of atoms contained in the single basin are bonded to each other with similar strength depending upon the value of the ELF. Figure 6 shows the isosurface of ELF taken at  $\chi_{\text{ELF}} = 0.68$ , for  $\text{Ga}_{30}$  and  $\text{Ga}_{31}$ . We note that for  $\text{Ga}_{30}$ , 26 atoms are connected via a single basin, whereas for  $\text{Ga}_{30}$ , the largest basin contains 12 atoms with other ‘‘fragmented’’ basins. This supports our earlier observation that  $\text{Ga}_{31}$  has significantly more similarly bonded atoms than  $\text{Ga}_{30}$ . Further evidence for the amorphous nature of  $\text{Ga}_{30}$  comes from the comparison of the entropies of these systems (figure not shown). As expected the entropy of amorphous structure ( $\text{Ga}_{30}$ ) rises rather sharply as compared to  $\text{Ga}_{31}$  (which is more ordered). Quite clearly, the amorphous

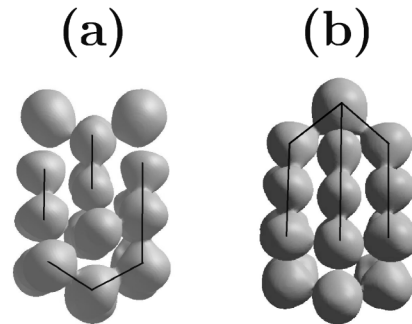


FIG. 6. The ELF of (a)  $\text{Ga}_{30}$  and (b)  $\text{Ga}_{31}$  at the value of  $\chi_{\text{ELF}} = 0.68$ . The black lines show connected basins.

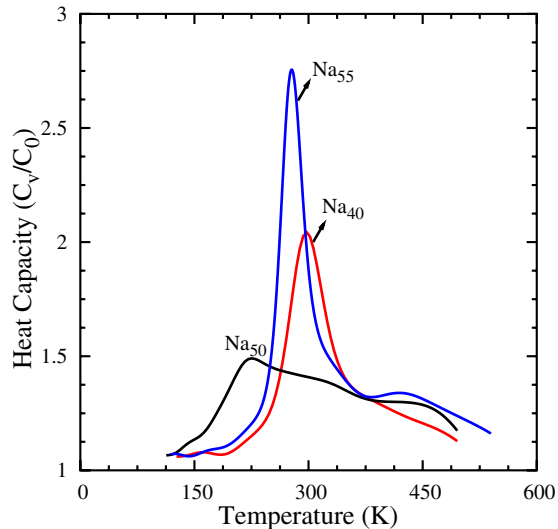


FIG. 7 (color online). The heat capacity of  $\text{Na}_{40}$ ,  $\text{Na}_{50}$ , and  $\text{Na}_{55}$  computed over 90 ps data.

nature leads to substantially large number of accessible states in case of  $\text{Ga}_{30}$  and is more by a factor of 10 as compared to  $\text{Ga}_{31}$  in the low energy region.

As mentioned earlier this size sensitive behavior is not unique to the gallium clusters reported here and has been observed in small Ga [9], Al [5], and Na [11] clusters. As an example we show the heat capacities of  $\text{Na}_n$  ( $n = 40, 50, 55$ ) clusters in Fig. 7. The change in the nature of the heat capacity as the cluster grows from  $\text{Na}_{40}$  to  $\text{Na}_{55}$  is quiet evident from Fig. 7. Our detailed analysis of the ground state geometries shows a direct correlation between the nature of the ground state and calculated heat capacities. It may be noted that  $\text{Na}_{55}$  is highly symmetric and very well ordered.  $\text{Na}_{40}$  is also ordered and has a basin containing a substantially large number of atoms, but  $\text{Na}_{50}$  is relatively disordered, which is clearly reflected in their heat capacities [19].

The main contribution of the present work is to bring out a definitive relationship between the local order in the cluster and its finite temperature behavior. As the cluster grows in size, it is very likely that it will evolve through a succession of such ordered and disordered geometries. In such cases the addition of one or a few atoms is likely to change (as demonstrated in this work) the nature of the ground state abruptly. Thus, the size sensitive nature of heat capacities is generic to small clusters and related to the evolutionary pattern seen in their ground state geometries. The evidence for this comes not only from gallium clusters but also from clusters of sodium and aluminum having very different nature of bonding.

Partial support from IFCPAR-CEFIPRA (Project No. 3104-2) New Delhi and the super computing facility from C-DAC is gratefully acknowledged.

- 
- [1] M. Schmidt, R. Kusche, B. v. Issendorff, and H. Haberland, *Nature (London)* **393**, 238 (1998); M. Schmidt, J. Donges, T. Hippler, and H. Haberland, *Phys. Rev. Lett.* **90**, 103401 (2003); H. Haberland, T. Hippler, J. Donges, O. Kostko, M. Schmidt, and B. von Issendorff, *Phys. Rev. Lett.* **94**, 035701 (2005).
  - [2] A. A. Shvartsburg and M. F. Jarrold, *Phys. Rev. Lett.* **85**, 2530 (2000).
  - [3] G. A. Breaux, R. C. Benirschke, T. Sugai, B. S. Kinnear, and M. F. Jarrold, *Phys. Rev. Lett.* **91**, 215508 (2003).
  - [4] G. A. Breaux, D. A. Hillman, C. M. Neal, R. C. Benirschke, and M. F. Jarrold, *J. Am. Chem. Soc.* **126**, 8628 (2004).
  - [5] G. A. Breaux, C. M. Neal, B. Cao, and M. F. Jarrold, *Phys. Rev. Lett.* **94**, 173401 (2005).
  - [6] K. Joshi, D. G. Kanhere, and S. A. Blundell, *Phys. Rev. B* **66**, 155329 (2002); **67**, 235413 (2003).
  - [7] S. Chacko, D. G. Kanhere, and S. A. Blundell, *Phys. Rev. B* **71**, 155407 (2005).
  - [8] S. Chacko, K. Joshi, D. G. Kanhere, and S. A. Blundell, *Phys. Rev. Lett.* **92**, 135506 (2004).
  - [9] S. Krishnamurty, S. Chacko, D. G. Kanhere, G. A. Breaux, C. M. Neal, and M. F. Jarrold, *Phys. Rev. B* **73**, 045406 (2006).
  - [10] S. Krishnamurty, K. Joshi, D. G. Kanhere, and S. A. Blundell, *Phys. Rev. B* **73**, 045419 (2006).
  - [11] M.-S. Lee, S. Chacko, and D. G. Kanhere, *J. Chem. Phys.* **123**, 164310 (2005).
  - [12] Vienna *ab initio* simulation package, Technische Universität Wien (1999); G. Kresse and J. Furthmüller, *Phys. Rev. B* **54**, 11 169 (1996).
  - [13] A. M. Ferrenberg and R. H. Swendsen, *Phys. Rev. Lett.* **61**, 2635 (1988); P. Labastie and R. L. Whetten, *Phys. Rev. Lett.* **65**, 1567 (1990).
  - [14] D. G. Kanhere, A. Vichare, and S. A. Blundell, *Reviews in Modern Quantum Chemistry*, edited by K. D. Sen (World Scientific, Singapore, 2001).
  - [15] A. Widmer-Cooper, P. Harrowell, and H. Fynewever, *Phys. Rev. Lett.* **93**, 135701 (2004).
  - [16] B. Silvi and A. Savin, *Nature (London)* **371**, 683 (1994).
  - [17] A. D. Becke and K. E. Edgecombe, *J. Chem. Phys.* **92**, 5397 (1990); J. K. Burdett and T. A. McCormick, *J. Phys. Chem. A* **102**, 6366 (1998).
  - [18] R. Rousseau and D. Marx, *Chem. Eur. J.* **6**, 2982 (2000); *Phys. Rev. Lett.* **80**, 2574 (1998); *J. Chem. Phys.* **111**, 5091 (1999); *Chem. Phys. Lett.* **295**, 41 (1998).
  - [19] These theoretically predicted heat capacities await experimental confirmation.